Study on the Relationships between Indentations made by Some Kinds of Indenters and Mechanical Properties of Cu Single Crystal

Eiichi SUKEDAI

Department of Mechanical Science, Okayama college of Science, Okayama, Japan

(Received September 16, 1975)

I Introduction

Since olden times, the indentation and percussion figures on the smooth and flat surface of metals and crystals are well known and interesting. Soon, the phenomena are used for determining crystallographic orientation of crystals [1], [2], for the study on the plasticity of glass [3], and especially, for the indentation hardness testing on metals and crystals.

Some kinds of indentation hardness testing methods have been widely used in the industry on account of the simple operation of tester and the easy preparation of specimens. However, the physical meaning of indentation hardness values is not distinct. Then, about polycrystalline materials, the relation between hardness value and ultimate tensile strength [4], [5] and the analysis of the indentation figures on the surface of material have been studied by crystallographic-plasticity [6], [7]; however the satisfactory results are not necessarily reached. One of the reasons, is that the details of deformation behaviours in the material arisen by indenter are not completely accounted for.

In this study, the figures on the surface and the three dimensional deformed-regions in the interior of indentations, which are made by some kinds of indenter on cube face of Cu single crystal, are mainly investigated by the dislocation etching. And the analysis of the deformation-behaviours of indentation and the elements for determing the hardness values are discussed.

II Experimental method

OFHC copper as material for the specimen is selected because of its distinct slip habits, its low stacking fault energy and its applicability of the dislocation etching method. Single crystals are glown by Bridgman method in vacuum

furnace. The surface normal of specimen for measuring indentation hardness values is [100] and the axes of specimens for tensile testing have the directions shown in Fig. 1. They are electro-polished. The initial dislocation density of specimens is about $5\times10^4/cm^2$, measured by dislocation etching method. For making indentations and testing hardness value, the micro hardness tester with some kinds of indenters is used. The indenters used are Vickers, Knoop and Conical-indenter with 30, 60, 90, 105, 144 and 180° apex angle. The loads used are 10, 50, 100, and 1000 g for conical indenter with 60° apex angle, 100 g for Vickers and Knoop indenter and 1000 g for others. Shimadzu autograph IS-2000 is used with strain rate $\dot{\varepsilon}\simeq10^{-2}$/sec for tensile testing. The temperatures for measuring the hardness values and tensile testing are 77, 210 and 298°K.

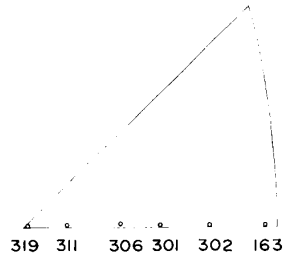

Fig. 1 Tensile axes of the specimens

The etchant used for dislocation etching is Livingston's one [8] for (111) face and the original one for cube face. The fine structures of slip lines are investigated with the replica method and electron microscope JEM 200.

III Results and Considerations

3-1 Original etchant for cube face of Cu single crystal

The etchant has the composition shown in Table 1. Fig. 2 shows the etch pits revealed by it. It is found that they have pyramidal shapes and similar sizes.

Table 1 Composition of the original etchant for Cube face of Copper

Distilled Water	28 cc
Ammonium Persulfate	13 cc
Ammonium Water	12 cc
Ammonium Bromide	3.6 cc

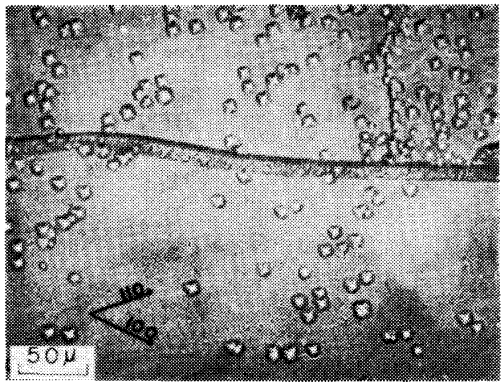

Fig. 2 Etch pits on cube face revealed by new etchant

One to one correspondence between the etch pit revealed by new etchant and dislocation is investigated as follows: on Livingston's etchant for (111) face, the correspondence are already recognized [9]. So, on same specimen, etch pit density on (111) face are measured by Livingston's etchant and it on cube face by new

one, and both densities are compared. The results are shown in Table 2 and it is found that density by the latter are barely smaller, however the orders of the value

Table 2 Comparison between etch pit density by Livingston's and Original etchant

Specimen	Etch pit density ($10^4/cm^2$)	
	by Livingston's one	by original one
No. 204	10	8.9
No. 205	13	11
No. 213	7.0	5.2

coincide with each other. Also as is shown in 3-2, the correspondence between the slip lines and the etch pit rows is very good. From these results it is found that the one to one correspondence between dislocations and etch pits by new etchant is almost established.

3 2 Analysis of indentations made by some kinks of indenters and a physical meaning of indentation hardness value

3-2-1 Indentation figure on the surface

Fig. 3 shows indentation made under the following conditions ; a conical indenter with 60° apex angle, a load of 1000g, a loading time for 60 sec, and 293°K. It shows 4-deformed regions like a petal along the [110] direction in coincidence with the crystallographic symmetry of specimen. Therefore, the following descriptions are limited to one quadrant surrounded by the [100] and the [010] directions from the indentation center on cube face. The slip lines perpendicular to the [110] direction remarkably appear in the whole deformed region, and those parallel to the [110] direction appear along the middle and the edges of the deformed region. These groups of slip lines are always observed in indentations made by conical indenters with different apex angles.

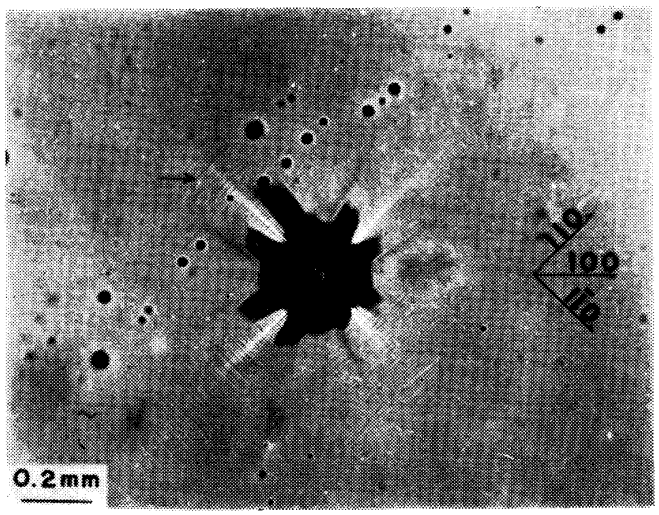

Fig. 3 Indentation with slip traces on cube face

Fig. 4 (A) and (B) show Vickers indentations, made under the following con-

ditions; the mounds of indenter parallel to the [100] and the [110], a load of 100 g, a loading time for 15 sec, and 293°K. The observed slip line and deformed regions are the same as Fig- 3. Therefore, it is found that the figures of indentations made by an indenter with nearly axial symmetry are almost the same.

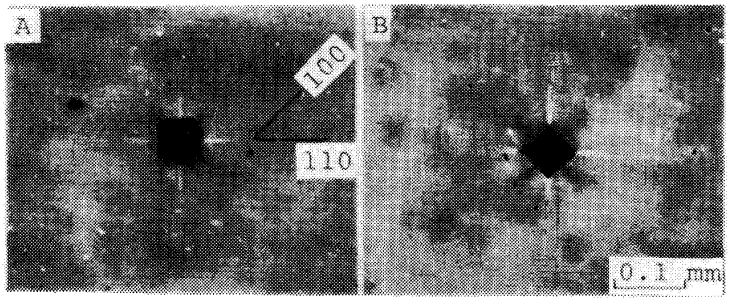

Fig. 4 Vickers indentation with slip traces: (A), the mound of indenter parallel to [100] and (B), to [110]

3-2-2 Distributions of dislocations on cube face for every depth

To obtain the three-dimensional informations of the deformed regions in indentation, the distributions of dislocations on cube face for every depth are studied by dislocation etching method. Fig. 5 shows the distributions of dislocations on the

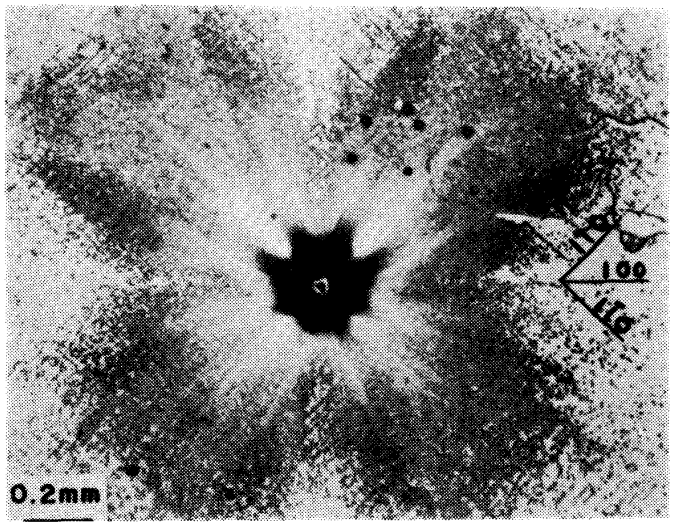

Fig. 5 Indentation with etch pits at surface level on cube face

surface layer. The rows of dislocations are correspondent with slip lines in Fig. 3, and dislocation densities along the middle and edge parts of the petal-like deformed region are very high. Fig. 6 shows the result at 0.07 mm depth, and the square-like high dislocation density region beneath the indenter and the three branched fork-like one outside the square are observed. Fig. 7 shows the result at 0.54 mm depth. From these and other results[11], the three dimensional high dislocation clustering zones in specimen are shown in Fig. 8. Each line through the base of fork-like

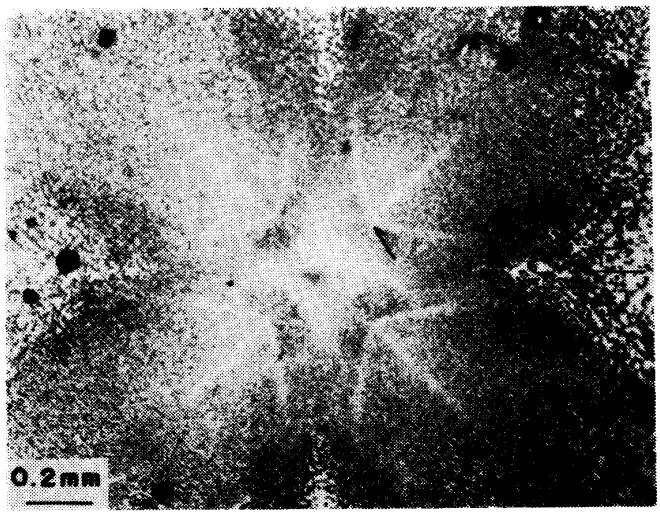

Fig. 6 Distribution of etch pits on (001) section at 0.07 mm depth

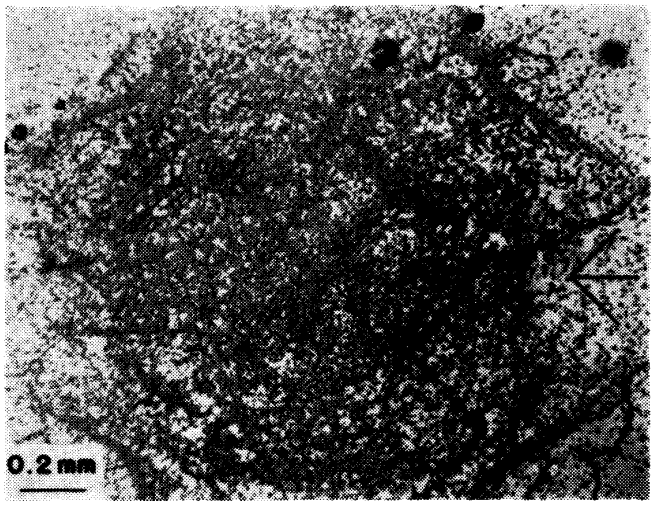

Fig. 7 Distribution of etch pits on (001) section at 0.54 mm depth

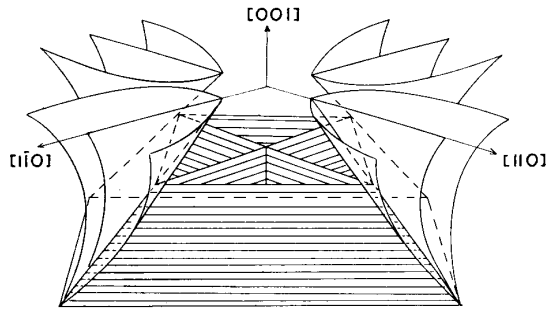

Fig. 8 Schematic diagram of the dislocation clustering zones. The region in the vicinity of the indentation is of more dislocation clustering

one inclines about 45° to the surface of specimen. The results mentioned above are observed in the indentations made by conical indenters with different apex angles[10]. Fig. 9 shows the distributions of dislocations in the indentations with Vickers indenter for each depth. Their high dislocation clustering regions are the same regardless of the direction of mound of Vickers indenter.

Because the observed high dislocation clustering regions have dislocation density

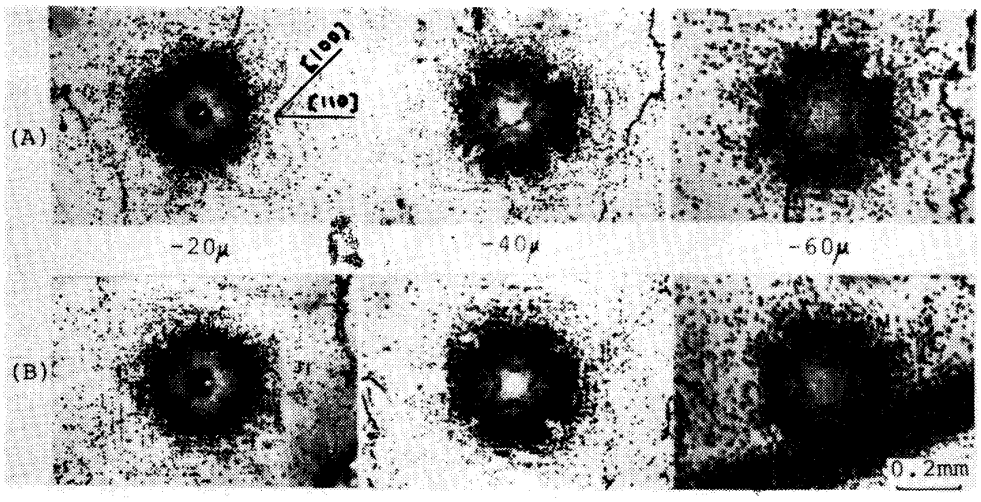

Fig. 9 Vickers indentations with etch pits at each depth: (A), diagonal of indenter parallels to [100], and (B), to [110]

more than $10^8/cm^2$ and they seem to be made by the interactions of the dislocations belonging to many slip systems while indentation is made, they seem to be strong obstacles to mobile dislocations. Therefore, these regions seem to be an important factor to determine the indentation hardness value. Also, these regions are always observed in indentations made by indenters with nearly axialsymetry. Therefore, the fact is thought to be a cause of the existence of mutual relationship between Vickers, Rockwell and Brinell hardness values.

3-2-3 Distributions of dislocations on (11$\bar{1}$)-sections

To consider the mechanism for making indentation and the properties of the high dislocation clustering regions, it is necessary to know the operating slip systems. So the distributions of dislocations on (11$\bar{1}$)-sections at different distances apart from the indentation center are studied by dislocation etching method.

The appearance on (11$\bar{1}$)-section through the indentation center is shown in Fig. 10. A and B corresponds the fork- and the square-like high dislocation clustering regions in Fig. 8, respectively. In the region C closer to surface and bounded by A, the dislocations on divergent slip planes are caused to happen and in the regions D and E side, those on convergent slip planes happen on the inner side. It is found that the slip planes on which dislocations occur in the surface- and inner-side are different. These results are found in indentations made by conical indenters with different apex angles [10].

Because these results are nearly the same as the distributions of dislocations on cube face in the indentation made with a Vickers indenter, the deformation mechanism of indentations on cube face made with the indenters of nearly axial

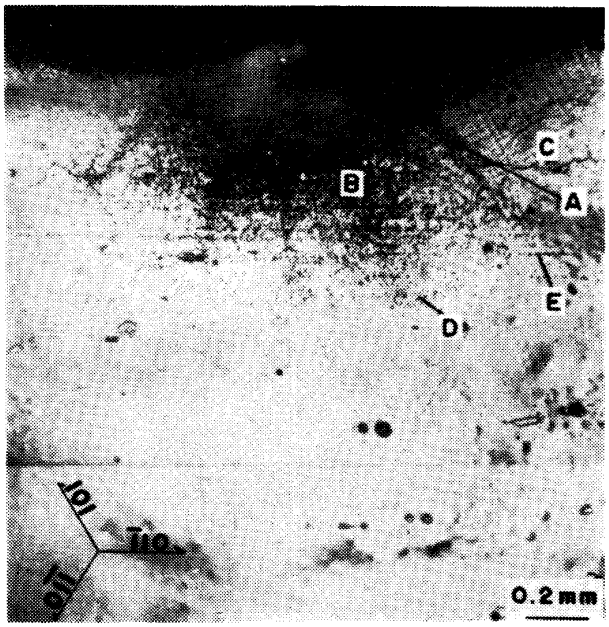

Fig. 10 Distribution of etch pits on (11i) section through the indentation centre: A, a cross-section of fork-like clustering zone; B, pyramidal clustering zone; C, etch pits configuration along operative divergent plane; D, convergent planes; E, (iii) convergent plane

symmetry seems to be the same as that of high dislocation clustering region in them.

3-2 4 Formation mechanism and contributions to hardness value of the high dislocation clustering regions

In the initiation of the deformation-process of indentation, the dislocations on convergent slip planes seem to be operate because of the observed results beneath the indenter shown in Fig. 10 and the results of investigation about indentations by spherical indenter [12], [13]. When the indenter penetrates inside farther, the dislocations on divergent and convergent slip planes seem to operate because of the results shown on C in Fig. 10. The Burgers vectors of dislocations on convergent slip planes are determined by

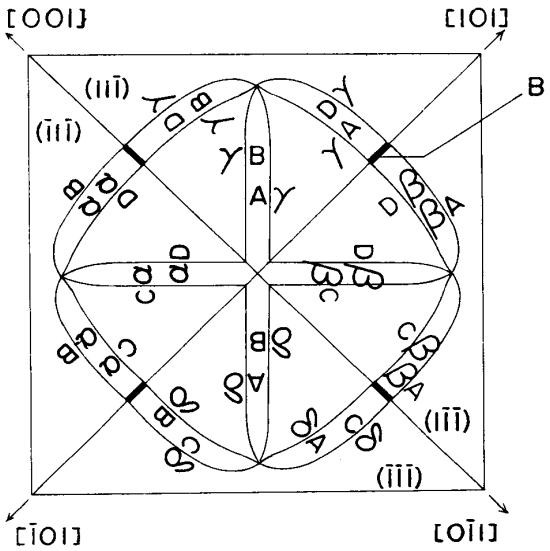

Fig. 11 Reaction of dissociated dislocation loops on convergent planes, B showing stair rod dislocation.

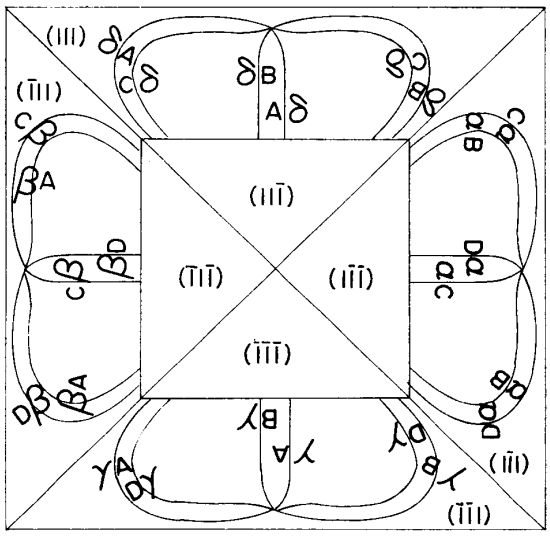

Fig. 12 Reaction of dissociated dislocation loops on divergent planes.

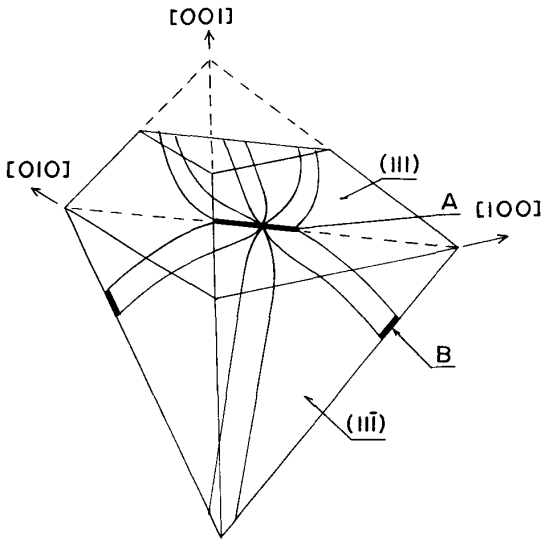

Fig. 13 Three dimensional model of dislocation configuration in the quadrant bounded by (100) and (010) plane.

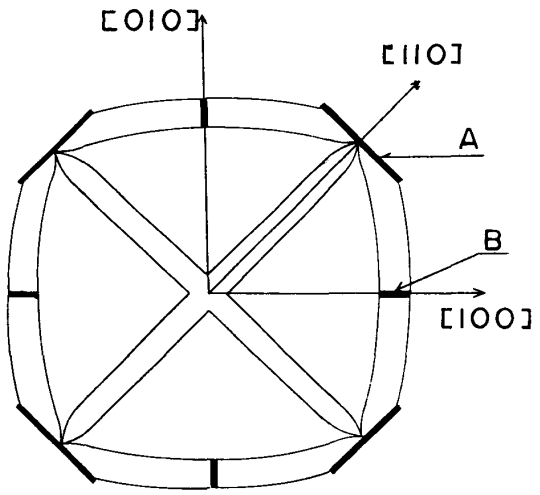

Fig. 14 Top view of whole figure consisting of 4-quadrants equivalent to Fig. 13. A and B, showing stair rod dislocations having the Burgers Vector $\delta\gamma$/BD and $\gamma\beta$/AD, respectively

assuming the flow of material to form the hollow; and those on the divergent slip planes, by assuming the flow to form the hill in the regions along the [110] direction. So referring to Hirth's results on the dislocation-interaction in face centered cubic metals[14],[15], the dislocation behaviours and interactions on divergent and convergent slip planes, and along the intersected line of two kinds of slip planes are considered. The results on convergent slip planes are shown in Fig. 11; those on divergent ones, in Fig. 12; and those along the intersected line of them, in Fig. 13. Fig. 14 shows the figure, projecting the results of Figs. 11, 12 and 13 on a cube face, and is similar to Fig. 7. Arrows A and B in Fig. 14 show the sessile dislocations having Burgers vector, a/3•⟨100⟩ and a/6•⟨013⟩, respectively. The former has lower self-energy than the perfect dislocation has, and its contribution to resistance on mobile dislocations seems larger[16]. It is thought that this fact causes the hardness value along the [100] direction on a cube face to be larger than that of [110].

3-3 Relationship between indentation hardness value and tensile strenght

3-3-1 Comparison of indentations made at 77, 210 and 293°K

Fig. 15 (a) and (b) show indentations made at 77 and 210°K, respectively, under the following conditions ; conical indenter with 60° apex angle, a load of 1000g and a loading time for 60 sec. The observed deformed regions and the groups of slip lines are the same as those observed in Fig. 3 and the distributions of dislocations in the specimen are the same as those observed in Figs. 5, 6 and 7.

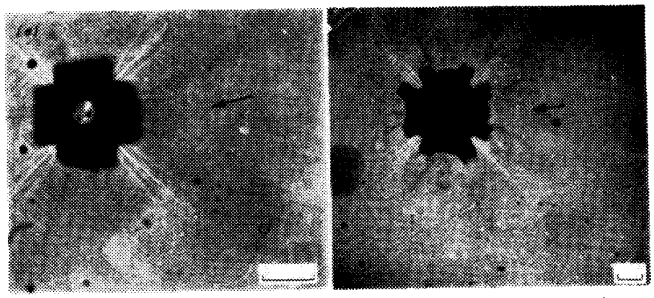

Fig. 15 Indentations with conical indenter on cube face (a) made at 77 K and (b) at 210 K (Scale=0.1 mm)

Fig. 16 is the fine structure of slip lines in the region denoted by an arrow in Fig. 3; and it shows the parallel slip lines with fine structure and wide and clear slip band (A), and the fragmentations (B). It is known by the study about the deformation behaviour on Cu single crystals that appearances of A and B are due to the contributions to cross-slipping of screw dislocations piled up at obstacles. Fig. 17 shows the fine structure of slip line on indentation at 77 K, and it has fine, straight and long slip lines. The observed region is correspondent to Fig. 16. Thus, it is found

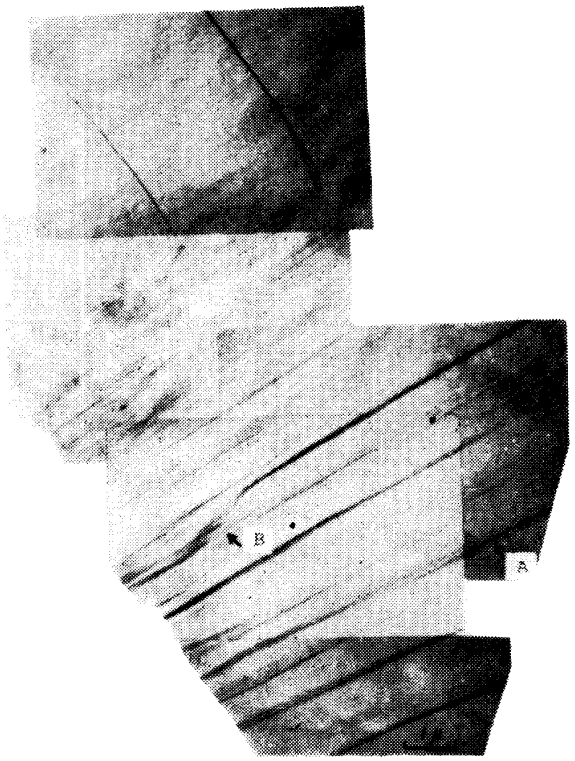

Fig. 16 Fine structures in slip traces of indentation made at 293°K.

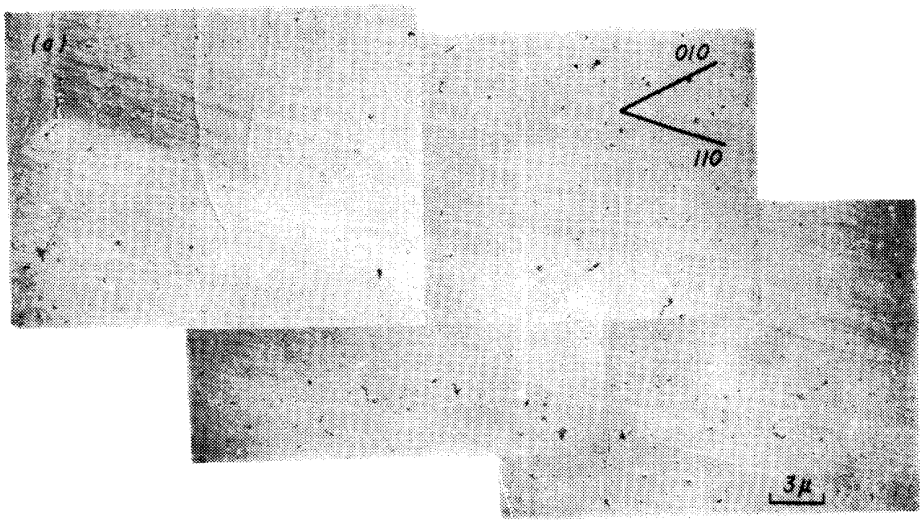

Fig. 17 Fine strucure in slip traces of indentation made at 77 K.

that the higher the deformation temperature is, the larger is the frequency of cross-slipping of screw dislocations piled up at the obstacles (eg.-in high dislocation clustering regions) in indentation.

3-3-2 Relationships between Knoop hardness value and τ_{III} value

It is well known that on the tensile tests of single crystals of FCC metals, the resolved shear stress-strain curves are generally divided into three stages shown in Fig. 18, and the beginning of stage III is closely connected to the cross-slipping of screw dislocations piled up at some obstacles[17]. Also, because the cross-slipping of screw dislocations depends upon a deformation temperature, it is considered that the indentation hardness values and the stress at the beginning of stage III, τ_{III}, show a similar inclination. So the relationship between these values are studied.

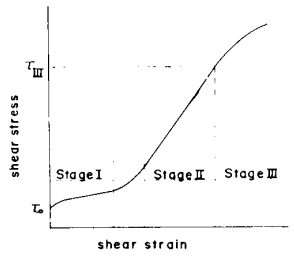

Fig. 18 Shear stress- shear strain curve of FCC metal

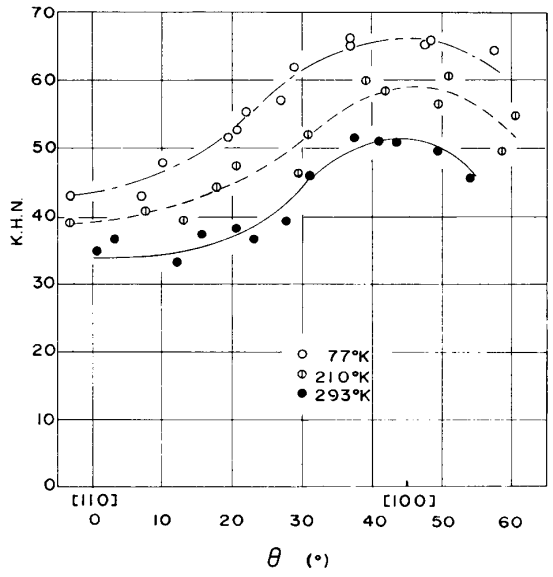

Fig. 19 Diargam of Knoop hardness number (K. H. N.) vs the angle θ of rotation of the short diagonal of Knoop indenter from [110] direction on cube face at 77, 210 and 293°K

Fig. 19 shows Knoop hardness values, measureda t 77, 210 and 293°K, at every 5° from the [110] to [100] direction on a cube face, and it is found that the lower the temperature is and the nearer the direction is to the [100], the higher are the values.

Generally, the strength of materials is dependent on crystallographic orientations and strain rate, etc. Also, of indentation hardness testing methods, Knoop indentation hardness values are determined by the deformation resistance of materials along the direction of short-diagonal of indenter[18], [19], and are most sensitively dependent on crystallographic orientations. Then, under the same conditions for measuring Knoop hardness values (at strain rate $\dot{\varepsilon} \fallingdotseq 10^{-2}$/sec, and at 77, 210 and 293°K), the tensile test of specimens having the axes shown in Fig. 1 are done. Fig. 20 (a), (b) and (c) show the results of specimen No 163, No 301 and No 319, respectively. Arrows (→) denote the beginning of stage III, and with a lower deformation tempereture, values of τ_{III} increase and its tendency is the

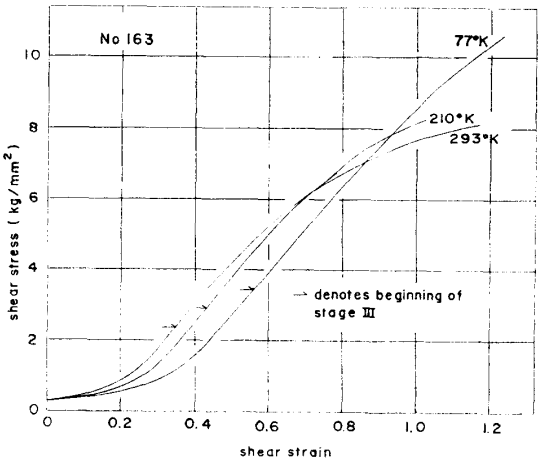

Fig. 20 (a) Shear stress-shear strain curves of No. 163 at 77, 210 and 293°K.

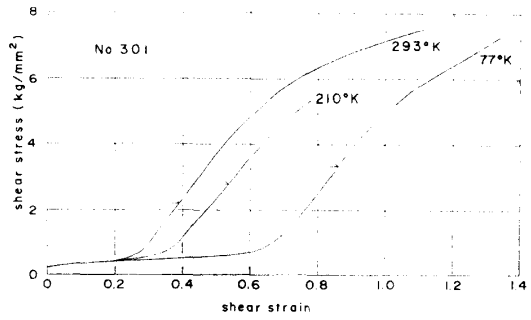

Fig. 20 (b) Shear stress-shear straln curves of No. 301 at 77, 210 and 293°K.

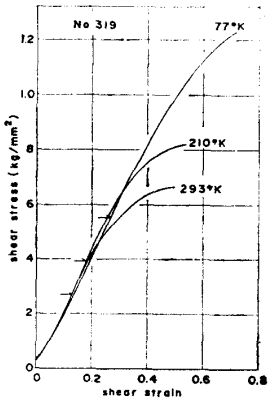

Fig. 20 (c) Shear stress-shear strain curves of No. 319 at 77, 210 and 293°K.

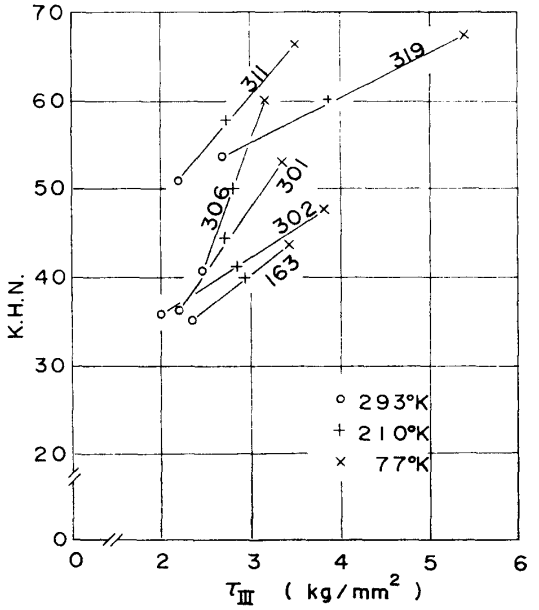

Fig. 21 The relationships between the Knoop hardness number at different directions on cube face and τ_{III} of Cu single crystals with the corresponding tensile axes at each temperature

same as the dependence of Knoop hardness values upon the temperature.

Fig. 21 shows variations of Knoop hardness values and τ_{III} on respectively dependent orientations at each deformation temperature and it is found that on each orientation, they seem to be linearly dependent on one another. This fact suggests that the temperature dependence of indentation hardness values is attributed by the same reason as that of τ_{III} in tensile test, and assuming from the results of tensile test[17], the resistances to deformations of indentation seem due to such obstacles to mobile dislocations as the high dislocation clustering regions and the sessile dislocations in the deformed regions of indentation.

IV Summary

In all indentations made by some indenters, the high dislocation clustering regions are always observed and similar. Because they are able to act as the resistance to mobile dislocations, they seem to be a main factor determing indentation hardness value and to be a cause of the mutual relationship between some indentation hardness values.

The high dislocation clustering regions are considered by the dislocation theory and the orientation dependence of indentation hardness values is found to be upon the sessile dislocations in those regions. Also, indentations at three different temperatures are compared and temperature dependences of Knoop hardness value and τ_{III} are considered. It is found that the temperature depedences seem to be upon the temperature dependence of cross slipping of screw dislocations piled up at obstacles.

V Acknowledment

The auther wishes to thank Dr. S. Yoshioka, Mr. M. Mera and Dr. Y. Nakayama of University of Osaka Prefecture for many useful discussions and encouragements.

References

(1) G. Tamman et al.,: Z. Metallkde., 18 (1926), 69.
(2) S. Yoshioka et al.,: J. Japan Inst Met., 21 (1959), 461.
(3) D. M. Marsch: Proc. Roy. Soc., A274 (1964), 420.
(4) R. Greaves et al.,: J. Iron and Steel Inst. 1 (1926), 335.
(5) B. Chalmers: Physical Metallurgy, John Wiley Sons, (1959), 220.
(6) F. W. Daniels et al.,: Trans ASM 41 (1949), 419.
(7) C. Brookes et al.,: Proc. Roy. Soc., A322 (1971), 73.
(8) J. D. Livingston: J. Appl. Phys., 31 (1961), 1071.
(9) K. Marukawa: J. Phys. Soc. Japan, 22 (1967), 499.
(10) S. Yoshioka et al.,: J. Japan Inst. Met., 37 (1973), 522.
(11) S. Yoshioka et al.,: ibid, 34 (1970). 1122.
(12) D. Tabor: The Hardness of Metals, Oxford London (1951).
(13) L. D. Dyer: Trans ASM 58 (1965), 620.
(14) J. P. Hirth: J. Appl. Phys., 32 (1961), 700.
(15) J. P. Hirth et al.,: Theory of Dislocations, MaGraw Hill (1968).
(16) F. C. Frank: Physica, 15 (1949), 31.
(17) S. Mader: Z. Physik, 149 (1957), 73.
(18) A. Seeger: Dislocations and Mechanical Properties of crystals; John Wiley Sons, (1957), 243.
(19) Y. Tozawa et al.,: J. Japan Soc. Tech. of Plasticity, 8 (1967), 631.
(20) P. L. Rittenhouse et al.,: Trans AIME 296 (1966), 496.